The effect of gauge length on tensile strength and Weibull modulus of polyacrylonitrile (PAN)- and pitch-based carbon fibers

Kimiyoshi Naito · Jenn-Ming Yang ·
Yoshihisa Tanaka · Yutaka Kagawa

Abstract Carbon fibers are widely used as a reinforcement in composite materials because of their high specific strength and modulus. Current trends toward the development of carbon fibers have been driven in two directions; ultrahigh tensile strength fiber with a fairly high strain to failure (∼2%), and ultrahigh modulus fiber with high thermal conductivity. Today, a number of ultrahigh strength polyacrylonitrile (PAN)-based (more than 6 GPa), and ultrahigh modulus pitch-based (more than 900 GPa) carbon fibers have been commercially available. In this study, the tensile strengths of PAN- and pitch-based carbon fibers have been investigated using a single filament tensile test at various gauge lengths ranging from 1 to 250 mm. Carbon fibers used in this study were ultrahigh strength PAN-based (T1000GB, IM600), a high strength PAN-based (T300), a high modulus PAN-based (M60JB), an ultrahigh modulus pitch-based (K13D), and a high ductility pitch-based (XN-05) carbon fibers. The statistical distributions of the tensile strength were characterized. It was found that the Weibull modulus and the average tensile strength increased with decreasing gauge length, a linear relation between the Weibull modulus, the average tensile strength and the gauge length was established on log–log scale. The results also clearly show that for PAN- and pitch-based carbon fibers, there is a linear relation between the Weibull modulus and the average tensile strength on log–log scale.

Introduction

Carbon fibers are widely used as a reinforcement in composite materials because of their high specific strength and modulus. Such composites have become a dominant material in the aerospace, automotive, and sporting goods industries [1–3]. Current trends toward the development of carbon fibers have been driven in two directions; ultrahigh tensile strength fiber with a fairly high strain to failure (∼2%), and ultrahigh modulus fiber with high thermal conductivity. Today, a number of ultrahigh strength PAN-based (more than 6 GPa), and ultrahigh modulus pitch-based (more than 900 GPa) carbon fibers have been commercially available.

Recently, Naito et al. [4, 5] characterized the tensile, flexural properties, and Weibull modulus of ultrahigh strength PAN-based, ultrahigh modulus pitch-based and high ductility pitch-based single carbon fibers, and concluded that the Weibull modulus under the flexural test was higher than that obtained under the tensile test. The differences in the Weibull modulus under flexural and tensile deformation of these fibers could be explained in terms of Weibull statistical theory and fracture behavior. The Weibull modulus is attributed to the nature and distribution of the flaws, which are present in the fibers. It is well-known that many defects in the carbon fiber are created during precursor manufacturing and subsequent heat treatment process. These include fibrillar misalignment,

K. Naito (✉) · Y. Tanaka
National Institute for Materials Science, Hybrid Materials Unit,
Composite Materials Group, 1-2-1 Sengen, Tsukuba, Ibaraki
305-0047, Japan
e-mail: NAITO.Kimiyoshi@nims.go.jp

J.-M. Yang
Department of Materials Science and Engineering, University
of California Los Angeles, Los Angeles, CA 90095-1595, USA

Y. Kagawa
Research Center for Advanced Science and Technology,
The University of Tokyo, 4-6-1 Komaba, Meguro-ku,
Tokyo 153-8904, Japan

ultramicropores, etc. [6]. In the three-point bending test, a much smaller volume of carbon fiber is subjected to the maximum stress than that in a tensile test. As a result, the probability of having critical flaws that contribute to failure is lower, leading to a higher Weibull modulus and flexural strength as well. This tendency was clearly observed for the high strength carbon fibers. However, for the high modulus fibers, the Weibull modulus in flexure was higher but the flexural strength was lower than its tensile properties. High modulus carbon fibers have quite low compressive and shear strengths. The flexural strength could be affected strongly by its low strength under compression and shear loading [5].

Another method to examine the interaction of flaws for the carbon fibers that contribute to failure is changing the gauge length under tensile test. The effects of gauge length on tensile strength of carbon fibers have been reported in the literature [7–12]. Jones et al. [13] conducted the tensile tests on carbon fibers with different gauge lengths and concluded that (1) The Weibull shape parameter was not dependent on the gauge length. (2) Relation between the tensile strength and the gauge length could be approximated by a straight line on log–log scale. (3) The slope of the straight line corresponded to the inverse of the Weibull shape parameter. On the contrary, Asloum et al. [14] indicated that the shape parameter depended on the gauge length and it did not coincide with the slope of regression line for the relation between the tensile strength and the gauge length.

In this study, tensile tests of single filaments at various gauge lengths for several commercially available high strength and ultrahigh strength PAN-based, high modulus PAN-based, ultrahigh modulus pitch-based, and high ductility pitch-based carbon fibers were performed. The effects of gauge length on tensile strength and Weibull modulus of PAN- and pitch-based carbon fibers were evaluated.

Experimental procedure

Materials

The carbon fibers used in this study were: (i) ultrahigh strength (T1000GB, IM600), high strength (T300), and high modulus (M60JB) PAN-based (ii) ultrahigh modulus (K13D) and high ductility (XN-05) pitch-based carbon fibers.[1] The T1000GB, T300, and M60JB PAN-based

carbon fibers were supplied from Toray Industries, Inc. The IM600 PAN-based carbon fiber was supplied from Toho Tenax Co., Ltd. The XN-05 pitch-based carbon fiber was supplied from Nippon Graphite Fiber Corp. and the K13D pitch-based carbon fiber was supplied from Mitsubishi Plastics, Inc.

The physical properties of PAN- and pitch-based carbon fibers are listed in Table 1. All the as-received fibers had been subjected to commercial surface treatments and sizing (epoxy compatible sizing).

Specimen preparation

Single filament carbon fiber specimens were prepared on the stage with the help of a stereoscope. A single filament was selected from carbon fiber bundles and cut perpendicular to the fiber axis by a razor blade. The diameter of the single carbon fiber, d_f was measured using a laser scanning microscope (Lasertec Corp., 1LM15W) before testing and a high resolution scanning electron microscope (JEOL, JSM-6500F) during the fractured surface observation. No difference was observed between two techniques. The measured fiber diameters, d_f are shown in Table 1 (average diameters and standard deviations are obtained from the same kind of all carbon fibers at various gauge lengths). All specimens were stored in a desiccator at 20 ± 3 °C and at $10 \pm 5\%$ relative humidity prior to testing.

Tensile test

Tensile tests of single carbon fibers were performed using a universal testing machine (Shimadzu, Table top type tester EZ-Test) with a load cell of 10 N. The tensile specimen was prepared by fixing the filament on a paper holder with an instant high viscosity type cyanoacrylate adhesive, as reported elsewhere [15, 16]. The specimen was set up to the testing machine using active gripping systems. To allow for ease of severing of the paper holder and to avoid the fracture during gripping of the shorter length samples ($L = 1$ and 5 mm), a scalpel was used to widen the slot [11]. The holder was cut into two parts, before testing. Plastic films were set on both sides of the carbon fiber filament, and water was filled between them to avoid

---

[1] In the previous investigation, the cross-sections of the T1000GB and IM600 PAN-based, and the K13D and XN-05 pitch-based fibers are almost circular. The cross-sections of the T300 and M60JB PAN-based fibers are distorted oval. The T1000GB, IM600, T300, and M60JB PAN-based, and the XN-05 pitch-based fibers have particulate or granular morphology. The K13D pitch-based fiber has a sheet-like

Footnote 1 continued

microstructure. The fractured surfaces of the T1000GB, IM600, T300, and M60JB PAN-based, and the XN-05 pitch-based carbon fibers show the initiation of failure from surface defects and a rough, rather poorly defined granular texture. However, the K13D pitch-based fiber obscures the initiation of failure and observes the crystallite sheets are a result of pull out at failure [4, 5].

Table 1 Mechanical and physical properties of PAN- and pitch-based carbon fibers

Fiber	Gauge length L (mm)	PAN-based				Pitch-based	
		T1000GB T1000GB-12000-40D	IM600 IM600-24k E30	T300 T300-3000-50A	M60JB M60JB-3000-50B	K13D K13D2U	XN-05 XN-05-30S
Filaments[a] (count)		12000	24000	3000	3000	2000	3000
Yield (Tex)[a] (g/1000 m)		485	830	198	103	365	410
Density[a] ρ (g/cm^3)		1.80	1.80	1.76	1.93	2.20	1.65
Tensile modulus[a] E_f (GPa)		294	285	230	588	935	54
Average tensile strength $\sigma_{f.ave}$ (GPa)	1	9.01 (0.79)	8.56 (0.73)	4.52 (0.46)	5.34 (0.57)	5.12 (0.85)	1.53 (0.18)
	5	7.71 (0.88)	6.98 (0.79)	3.95 (0.46)	4.60 (0.56)	4.00 (0.82)	1.34 (0.17)
	12.5	6.27 (0.98)	5.79 (0.83)	3.49 (0.46)	4.06 (0.61)	3.64 (0.87)	1.21 (0.16)
	25	5.69[b] (1.02)	5.20 (0.87)	3.20[b] (0.49)	3.38[b] (0.63)	3.21[b] (0.81)	1.10[b] (0.15)
	50	5.03 (0.90)	4.39 (0.79)	–	–	3.20 (0.86)	0.98 (0.13)
	100	4.81 (0.88)	–	–	–	–	–
	250	4.46 (0.84)	–	–	–	–	–
Diameter d_f (μm)		5.06 (0.22)	5.22 (0.30)	7.37 (0.34)	5.13 (0.36)	11.68 (0.63)	9.35 (0.55)
Average flexural strength[c] $\sigma_{f.ave(flexure)}$ (GPa) (span length L = 200 μm)		8.19 (0.72)	–	5.20 (0.47)	3.92 (0.35)	2.09 (0.18)	3.04 (0.26)

[a] Producer's data sheet

T1000GB, T300, and M60JB: Catalog for TORAYCA, Toray Industries, Inc. (Toray), High performance carbon fiber Torayca in Japanese. 2004

IM600: Catalog for Toho Tenax Filament, Toho Tenax Co.,Ltd., Properties of Filament. 2008

XN-05: Catalog for GRANOC Yarn, Nippon Graphite Fiber Corp. (NGF), Technical data XNL

K13D: Catalog for DIALEAD, Mitsubishi Plastics, Inc., High performance coal tar pitch carbon fiber. 2009

[b] Single filament tensile data (25-mm gauge length) from previous investigation [4]

[c] Single filament flexure data (200-μm span length) from previous investigation [5]

( ) indicate standard deviations

secondary damage of the carbon fiber. The gauge lengths, L of 1, 5, 12.5, 25, 50, 100, and 250 mm and crosshead speed of 0.5 mm/min were applied. All tests were conducted under the laboratory environment at room temperature (at 23 ± 3 °C and $50 \pm 5\%$ relative humidity). Twenty specimens were tested for all carbon fibers.[2] The fracture morphologies of these carbon fibers were examined using a high resolution scanning electron microscope (JEOL, JSM-6500F) at an operating voltage of 5 kV.

Results

For all the carbon fibers, the stress applied to the specimen was linearly proportional to the strain until failure. The tensile fracture surfaces of the PAN-based (T1000GB,

T300, and M60JB) and the pitch-based (K13D and XN-05) carbon fibers at gauge length of 25 mm were showed in our previous report [4] and those including the IM600 PAN-based carbon fibers at various gauge lengths ranging from 1 to 250 mm were also observed in this study. Scanning electron microscope (SEM) micrographs of transverse cross-sectional views for the tensile fractured surfaces of the T1000GB PAN-based carbon fibers at various gauge lengths ranging from 1 to 250 mm are shown in Fig. 1. The failure initiation sites were clearly observed and similar fracture characteristics were observed in the IM600, T300, M60JB, and XN-05 carbon fibers. For the K13D carbon fiber at various gauge lengths ranging from 1 to 50 mm, the failure initiation sites were obscured. Morimoto et al. [17] indicated the gauge length dependence on the Weibull parameters of the silicon carbide (SiC: Tyranno ZMI Si–Zr–C–O) fiber provided biased estimation and classified the fracture surfaces into the characteristic fracture patterns. In this study, however, the fracture morphological differences among the gauge lengths for all PAN- and pitch-based carbon fibers were not observed and it was difficult to classify the fracture surfaces of all carbon fibers

---

[2] In this testing procedure, all carbon fiber filaments did not shatter and all specimens were recovered. However, a few (10–20%) samples failed in the edge of the holder or outside of the gauge section. Fractures that initiated inside the gauge section of a fiber and the samples that recovered the fracture surfaces were counted.

into the characteristic patterns. The tensile strength, σ_f is calculated using:

$$\sigma_f = \frac{P_{max}}{\left(\frac{\pi d_f^2}{4}\right)} \qquad (1)$$

where P_{max} is the maximum fracture load and d_f is the individual measured diameter of the single carbon fiber.

The average tensile strengths ($\sigma_{f.ave}$) at various gauge lengths are shown in Table 1. The results showed that the ultrahigh strength PAN-based T1000GB and IM600 fibers at gauge length of 1 mm have average tensile strength, $\sigma_{f.ave}$ of 8.98 ± 0.80 and 8.64 ± 0.78 GPa, respectively. The ultrahigh modulus pitch-based K13D fiber at gauge length of 1 mm has an average tensile strength, $\sigma_{f.ave}$ of 5.12 ± 0.85 GPa. The high ductility pitch-based XN-05 fiber at gauge length of 1 mm has an average tensile strength, $\sigma_{f.ave}$ of 1.53 ± 0.18 GPa. For each type of carbon fiber, the average tensile strength decreased with increasing the gauge length.

The results shown in Table 1 clearly indicate that there is an appreciable scattering of tensile strength for these carbon fibers. The statistical distribution of fiber strengths is usually described by means of the Weibull equation [18]. The two-parameter Weibull distribution is given by

$$P_F = 1 - \exp\left[-\frac{L}{L_0}\left(\frac{\sigma_f}{\sigma_0}\right)^{m_f}\right] \qquad (2)$$

where P_F is the cumulative probability of failure of a carbon fiber of length L at applied tensile strength σ_f, m_f is the Weibull modulus (Weibull shape parameter) of the carbon fiber, σ_0 a Weibull scale parameter (characteristic stress), and L_0 a reference gauge length. The cumulative probability of failure, P_F, under a particular stress is given by

$$P_F = \frac{i}{n+1} \qquad (3)$$

where i is the number of fibers that have broken at or below a stress level and n is the total number of fibers tested. Rearrangement of the two-parameter Weibull statistical distribution expression (Eq. 2) gives the following:

$$\ln\left(\ln\left[\frac{1}{1-P_F}\right]\right) = m_f \ln(\sigma_f) - m_f \ln\left(\sigma_0 \left(\frac{L_0}{L}\right)^{\frac{1}{m_f}}\right) \qquad (4)$$

Hence the Weibull modulus, m_f can be obtained by linear regression from a Weibull plot of Eq. 4.

Figure 2 shows the Weibull plots of ultrahigh tensile strength PAN-based (T1000GB, IM600), ultrahigh tensile modulus pitch-based (K13D), high ductility pitch-based (XN-05), high strength PAN-based (T300), and high modulus PAN-based (M60JB) carbon fibers at various gauge lengths ranging from 1 to 50 mm. For the fibers at

the gauge length of 1 mm, the Weibull modulus, m_f for the T1000GB, IM600, K13D, XN-05, T300, and M60JB fibers were calculated to be 11.92, 11.68, 6.38, 8.95, 10.39, and 9.87, respectively. The results clearly show that ultrahigh modulus pitch-based (K13D) carbon fiber has the lowest Weibull modulus, m_f, while the ultrahigh tensile strength PAN-based (T1000GB) carbon fibers has the highest Weibull modulus, m_f. For the fibers at the gauge length of 5 mm, the Weibull modulus, m_f for the T1000GB, IM600, K13D, XN-05, T300, and M60JB fibers were calculated to be 9.24, 9.43, 5.24, 8.45, 9.06, and 8.83, respectively. The Weibull modulus, m_f of the T1000GB, IM600, XN-05, T300, and M60JB fibers are almost similar, although ultrahigh modulus pitch-based (K13D) carbon fiber has the lowest Weibull modulus, m_f. For the fibers at the gauge length of 12.5, 25, and 50 mm, ultrahigh modulus pitch-based (K13D) carbon fiber has the lowest Weibull modulus, m_f, while the high ductility pitch-based (XN-05) carbon fibers has the highest Weibull modulus, m_f.

Figure 3 shows the Weibull plots of ultrahigh tensile strength PAN-based (T1000GB) carbon fibers at various gauge lengths ranging from 1 to 250 mm. The Weibull modulus, m_f of the T1000GB fibers at gauge lengths, L of 1, 5, 12.5, 25, 50, 100, and 250 mm were calculated to be 11.92, 9.24, 6.79, 5.86, 5.78, 5.72, and 5.67, respectively. The results clearly show that both tensile strength, σ_f and the Weibull modulus, m_f decreased with increasing the gauge length, L. This trend was observed for all PAN- and pitch-based carbon fibers. A threshold of the tensile strength was observed. The influence of threshold stress on the estimation of the Weibull statistics was discussed by Lu et al. [19, 20]. It was concluded that the two-parameter Weibull distribution is still a preferred choice, if test specimens are limited in number and threshold stress is not too large. As a result, the two-parameter Weibull distribution was applied in this study. The (Weibull plot estimated) Weibull modulus (m_f) of PAN- and pitch-based carbon fibers at various gauge lengths is summarized in Table 2.

The existing versions of standards for statistical analysis of ceramic strength data used the Maximum likelihood (ML) method for parameter estimation [21–25]. In this study, the Weibull parameters (the Weibull modulus and the Weibull scale parameter) were also estimated from the experimental data where all failures originate from a single flaw population (a single failure mode) using the ML method for comparison. The ML estimated Weibull modulus of PAN- and pitch-based carbon fibers at various gauge lengths are also summarized in Table 2. The parameter estimate of the Weibull modulus generally exhibits statistical bias. The amount of statistical bias depends on the number of specimens. An unbiased estimate of the Weibull modulus is obtained using the ML estimated

Fig. 1 SEM micrographs of the tensile fractured surfaces showing the transverse cross-section structure of T1000GB PAN-based carbon fibers at various gauge lengths ranging from 1 to 250 mm. **a** gauge length of 1 mm, **b** gauge length of 5 mm, **c** gauge length of 12.5 mm, **d** gauge length of 25 mm, **e** gauge length of 50 mm, **f** gauge length of 100 mm, and **g** gauge length of 250 mm
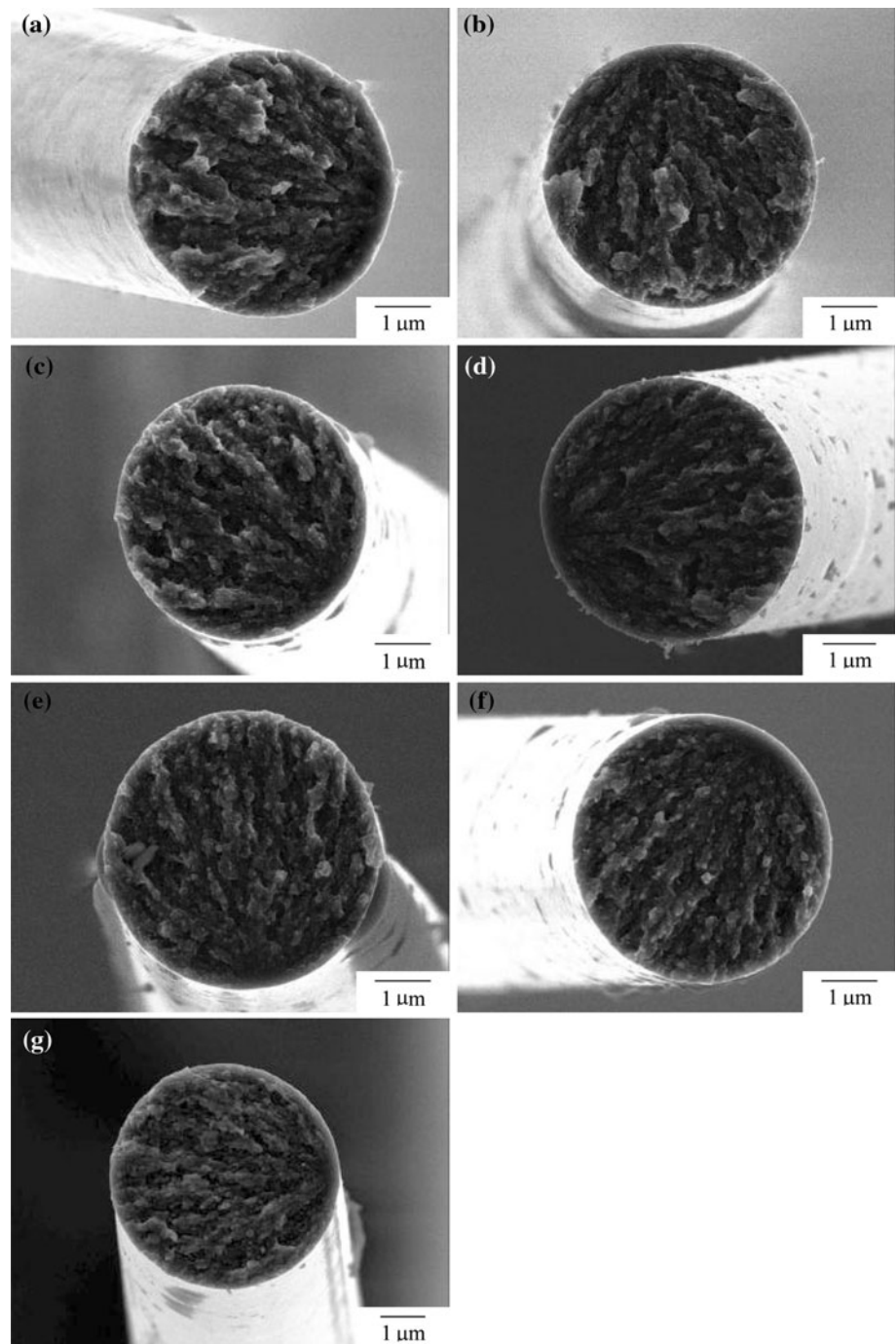
Weibull modulus and the unbiasing factors (=0.931) (see, Table 2). The confidence bounds quantify the uncertainty associated with a point estimate of a population parameter. The 90% confidence bound on the ML estimated Weibull modulus is obtained using the 5 and 95% distribution of the ratio, q for the Weibull modulus. The upper ($q_{0.05} = 0.791$) and the lower ($q_{0.95} = 1.449$) bounds are shown in Table 2. The Weibull plot estimated Weibull modulus is almost similar to the ML estimated Weibull modulus (including unbiased estimate). Hereafter, the Weibull plot

estimated Weibull modulus and the confidence bounds on the ML estimated Weibull modulus was used.

Discussion

Weibull modulus versus gauge length

It has been reported that single modal Weibull parameters provided biased estimation on the gauge length dependence

Fig. 2 Weibull plots for PAN- and pitch-based carbon fibers at various gauge lengths. *Open circle* T300, *open square* T1000GB, *open diamond* IM600, *open triangle* M60JB PAN-based, and *filled circle* XN-05, *filled diamond* K13D pitch-based carbon fibers. **a** gauge length of 1 mm, **b** gauge length of 5 mm, **c** gauge length of 12.5 mm, **d** gauge length of 25 mm, and **e** gauge length of 50 mm
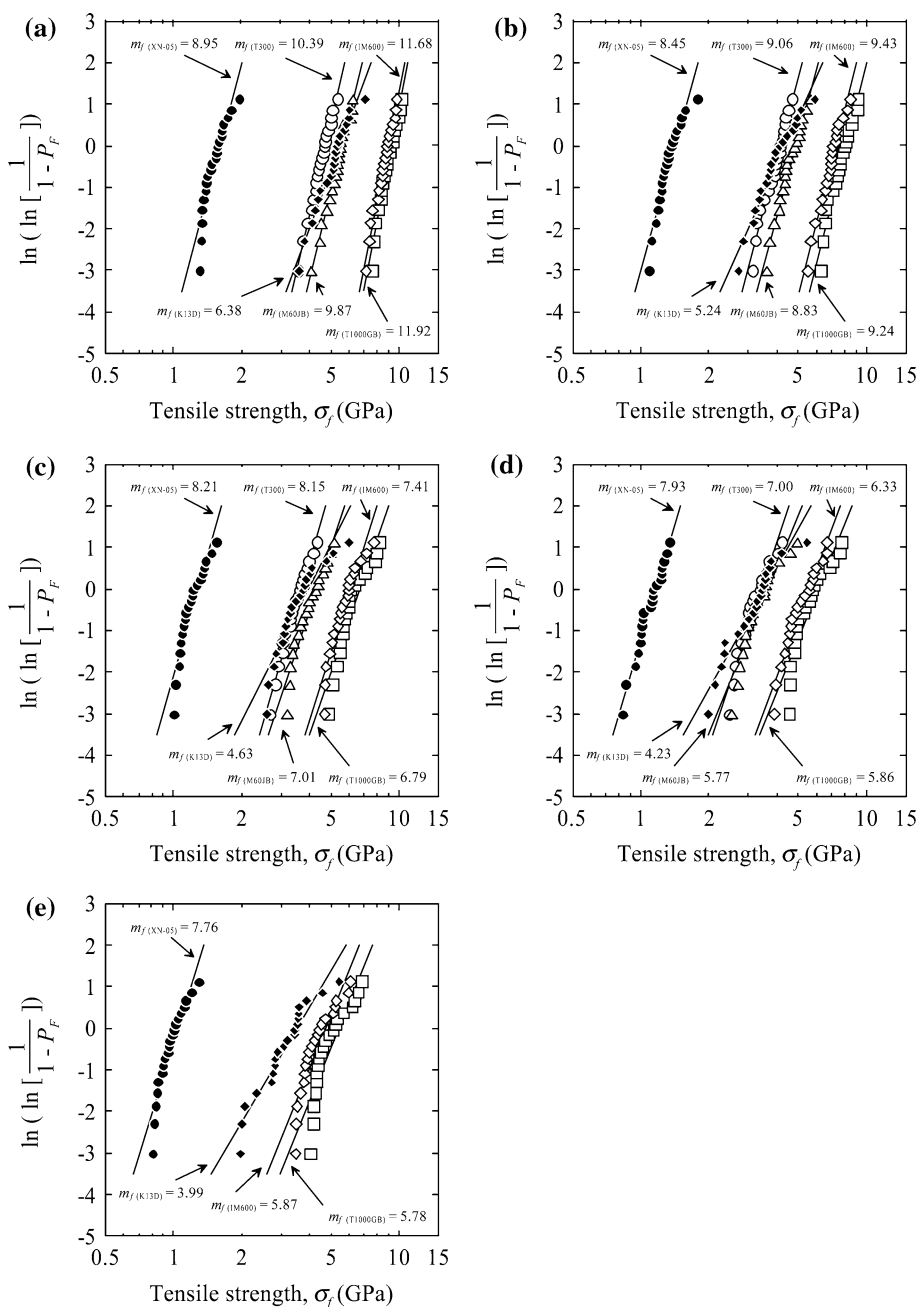
for some ceramic fibers [26, 27]. A weakest link hypothesis on the bias is that the density of critical defects is very small and fracture probability of shorter gauge length samples distributes in discrete manner, which makes the Weibull parameters dependent on the gauge length.

Figure 4 shows the relations between the Weibull modulus, m_f and the gauge length, L of ultrahigh tensile strength PAN-based (T1000GB, IM600), ultrahigh tensile modulus pitch-based (K13D), high ductility pitch-based (XN-05), high strength PAN-based (T300), and high modulus PAN-based (M60JB) carbon fibers. The results clearly showed that when the gauge length is less than

100 mm, the Weibull modulus of all carbon fibers increased with decreasing the gauge length and there is a linear relation between the Weibull modulus and the gauge length on log–log scale. Thus, the Weibull modulus is given by

$$m_f = \left(\frac{L}{L_0}\right)^{\alpha} \tag{5}$$

where, L_0 and α are the characteristic length and the length factor of Weibull modulus.

The slop, α strongly depended on the strength, modulus and structure of the carbon fibers (see Materials). The
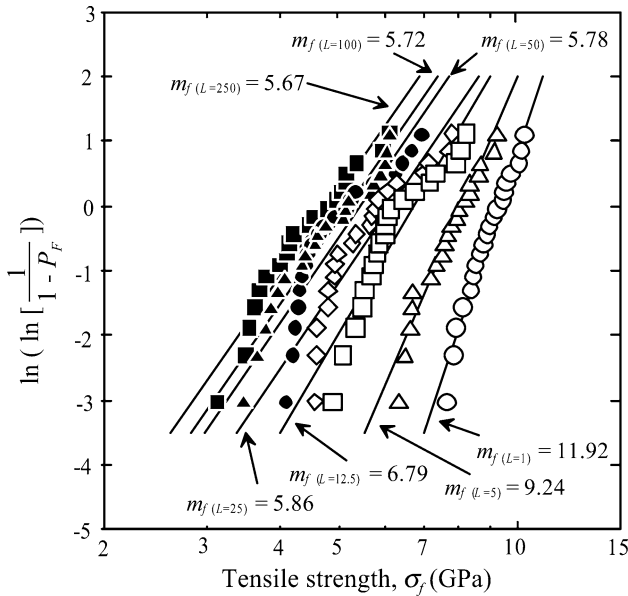
Fig. 3 Weibull plots for ultrahigh tensile strength PAN-based (T1000GB) carbon fibers at various gauge lengths. *Open circle* 1 mm, *open triangle* 5 mm, *open square* 12.5 mm, *open diamond* 25 mm, *filled circle* 50 mm, *filled triangle* 100 mm, and *filled square* 250 mm gauge lengths

highest $|\alpha|$ was observed for the ultrahigh strength T1000GB PAN-based fiber and the lowest $|\alpha|$ was observed for the high ductility (low strength and modulus) XN-05 pitch-based fiber. The $|\alpha|$ of ultrahigh strength T1000GB PAN-based fiber was higher than that of high strength T300 PAN-based fiber and it was clear observed the strength dependence of the slop. The $|\alpha|$ of the high modulus M60JB PAN-based fiber was higher than that of the high strength T300 PAN-based fiber, while the tensile strength of the T300 fiber was almost similar to that of the M60JB fiber (modulus dependence). The $|\alpha|$ of the ultrahigh modulus K13D pitch-based fiber was lower than that of the high modulus M60JB PAN-based fiber (structure dependence).

Tensile strength versus gauge length

Figure 5 shows the relation between the average tensile strength, $\sigma_{f.ave}$ and the gauge length, L of ultrahigh tensile strength PAN-based (T1000GB, IM600), ultrahigh tensile modulus pitch-based (K13D), high ductility pitch-based (XN-05), high strength PAN-based (T300), and high modulus PAN-based (M60JB) carbon fibers. The results clearly showed that the average tensile strength increased with decreasing the gauge length and there is a linear relation between the average tensile strength and the gauge length on log–log scale.

The characteristic fiber strength σ_L ($P_F = 0.632$) of gauge length L is related to the characteristic stress (the

Weibull scale parameter) σ_0 at characteristic length L_0 by the strength-length relationship [28]

$$\sigma_L = \sigma_0 \left(\frac{L_0}{L}\right)^{\frac{1}{m_f^*}} \tag{6}$$

There is a linear relation between the average tensile strength and the gauge length on log–log scale, as shown in Fig. 5. σ_L is replaced with the average tensile strength ($\sigma_{f.ave}$) in Eq. 6.

$$\sigma_{f.ave} = \sigma_0 \left(\frac{L_0}{L}\right)^{\frac{1}{m_f^*}} \tag{7}$$

The slope of the straight line corresponds to the inverse of the Weibull shape parameter (Weibull modulus), m_f^* as shown in Eq. 7. The Weibull shape parameters, m_f^* of the T1000GB, IM600, T300, M60JB, K13D, and XN-05 fibers were calculated to be 5.48, 6.27, 7.63, 5.31, 7.36, and 8.23. For the T1000GB, IM600, T300, M60JB, and XN-05 fibers, the Weibull modulus of tensile strength at gauge length of 25 mm were found to be 5.86, 6.33, 7.00, 5.77, and 7.93. The shape parameters obtained from the relation between the average tensile strength and the gauge length were similar to that of tensile strength at gauge length of 25 mm, while for the K13D fiber, the shape parameters obtained from the relation between the average tensile strength and the gauge length was higher than that of tensile strength at gauge length of 25 mm. The differences m_f^* among the fibers also depends on the strength, modulus, and structure of the carbon fibers (see Materials). The highest m_f^* was observed for the high ductility (low strength and low modulus) XN-05 pitch-based fiber and the lowest m_f^* was observed for the high modulus M60JB PAN-based fiber.

Weibull modulus versus tensile strength

To account for this decoupling of the scalings, a generalized Eq. 2 has been proposed as

$$P_F = 1 - \exp\left[-\left(\frac{L}{L_0}\right)^{\frac{m_f}{m_f^*}}\left(\frac{\sigma_f}{\sigma_0}\right)^{m_f}\right]$$

$$= 1 - \exp\left[-\left(\frac{L}{L_0}\right)^{\frac{\left(\frac{L}{L_0}\right)^\alpha}{m_f^*}}\left(\frac{\sigma_f}{\sigma_0}\right)^{\left(\frac{L}{L_0}\right)^\alpha}\right] \tag{8}$$

that introduces the additional parameter $\frac{m_f}{m_f^*}$ into the distribution. The length scaling of Eq. 7 is then modified

$$\sigma_{f.ave} = \sigma_0 \left(\frac{L_0}{L}\right)^{\frac{1}{m_f^*}} = \sigma_0 \left(\frac{L_0}{L}\right)^{\frac{\left(\frac{L}{L_0}\right)^\alpha}{m_f m_f^*}} \tag{9}$$

Table 2 Weibull modulus of PAN- and pitch-based carbon fibers

PAN-based

Fiber	Gauge length L (mm)	T1000GB (T1000GB-12000-40D)					IM600 (IM600-24k E30)				
		Weibull plot	Maximum likelihood (ML)	Unbiased estimate for ML	Upper bound for ML	Lower bound for ML	Weibull plot	Maximum likelihood (ML)	Unbiased estimate for ML	Upper bound for ML	Lower bound for ML
Weibull modulus m_f	1	11.92	12.71	11.83	16.06	8.77	11.68	13.25	12.34	16.76	9.15
	5	9.24	9.89	9.21	12.50	6.82	9.43	9.84	9.16	12.43	6.79
	12.5	6.79	6.64	6.18	8.39	4.58	7.41	7.10	6.61	8.97	4.90
	25	5.86[a]	5.78	5.38	7.31	3.99	6.33	6.63	6.17	8.38	4.57
	50	5.78	5.80	5.40	7.33	4.00	5.87	5.72	5.32	7.23	3.95
	100	5.72	6.37	5.93	8.06	4.40			–		
	250	5.67	5.85	5.44	7.39	4.03			–		
Weibull modulus $m_{f(flexure)}$ (span length, L = 200 µm)		11.71[b]	11.96	11.14	15.13	8.26			–		

PAN-based

Fiber	Gauge length L (mm)	T300 (T300-3000-50A)					M60JB (M60JB-3000-50B)				
		Weibull plot	Maximum likelihood (ML)	Unbiased estimate for ML	Upper bound for ML	Lower bound for ML	Weibull plot	Maximum likelihood (ML)	Unbiased estimate for ML	Upper bound for ML	Lower bound for ML
Weibull modulus m_f	1	10.39	11.34	10.56	14.34	7.83	9.87	11.12	10.35	14.05	7.67
	5	9.06	10.66	9.92	13.48	7.36	8.83	9.34	8.69	11.81	6.44
	12.5	8.15	8.46	7.87	10.69	5.84	7.01	7.43	6.92	9.40	5.13
	25	7.00[a]	6.96	6.48	8.79	4.80	5.77[a]	5.39	5.01	6.81	3.72
	50			–					–		
	100			–					–		
	250			–					–		
Weibull modulus $m_{f(flexure)}$ (span length, L = 200 µm)		11.59[b]	12.60	11.73	15.93	8.69	11.67[b]	11.95	11.13	15.11	8.25

Table 2 continued

Pitch-based

Fiber	Gauge length L (mm)	K13D (K13D2U)					XN-05 (XN-05-30S)				
		Weibull plot	Maximum likelihood (ML)	Unbiased estimate for ML	Upper bound for ML	Lower bound for ML	Weibull plot	Maximum likelihood (ML)	Unbiased estimate for ML	Upper bound for ML	Lower bound for ML
Weibull modulus m_f	1	6.38	6.54	6.09	8.27	4.52	8.95	8.57	7.98	10.84	5.92
	5	5.24	5.19	4.83	6.56	3.58	8.45	7.67	7.14	9.70	5.29
	12.5	4.63	4.23	3.94	5.35	2.92	8.21	7.98	7.42	10.08	5.50
	25	4.23[a]	4.10	3.82	5.19	2.83	7.93[a]	8.79	8.18	11.11	6.06
	50	3.99	3.92	3.65	4.96	2.71	7.76	7.40	6.89	9.35	5.11
	100			–					–		
	250			–					–		
Weibull modulus $m_{f(flexure)}$ (span length, $L = 200$ μm)		11.79[b]	13.02	12.12	16.46	8.98	11.66[b]	12.01	11.18	15.18	8.29

[a] Single filament tensile data (25-mm gauge length) from previous investigation [4]

[b] Single filament flexure data (200-μm span length) from previous investigation [5]
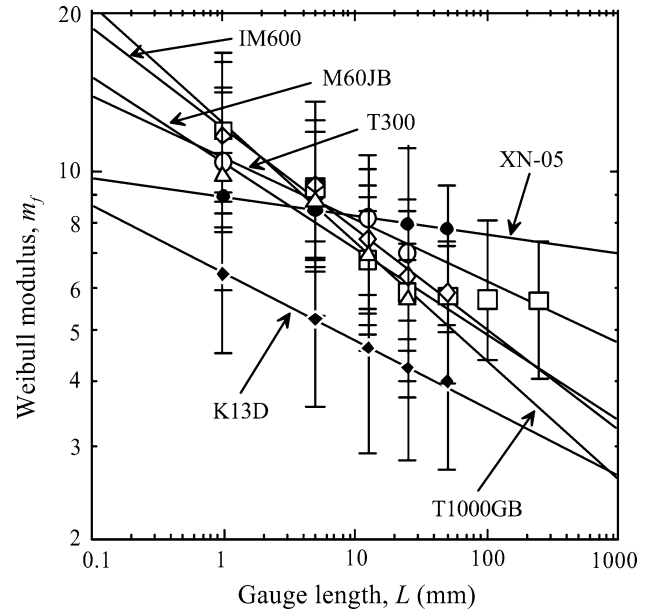
Fig. 4 Relation between the Weibull modulus and the gauge length of PAN- and pitch-based carbon fibers. *Open circle* T300, *open square* T1000GB, *open diamond* IM600, *open triangle* M60JB PAN-based and *filled circle* XN-05, *filled diamond* K13D pitch-based carbon fibers. $\alpha = -0.117$ (T300), -0.225 (T1000GB), -0.191 (IM600), -0.164 (M60JB), -0.036 (XN-05), and -0.128 (K13D)
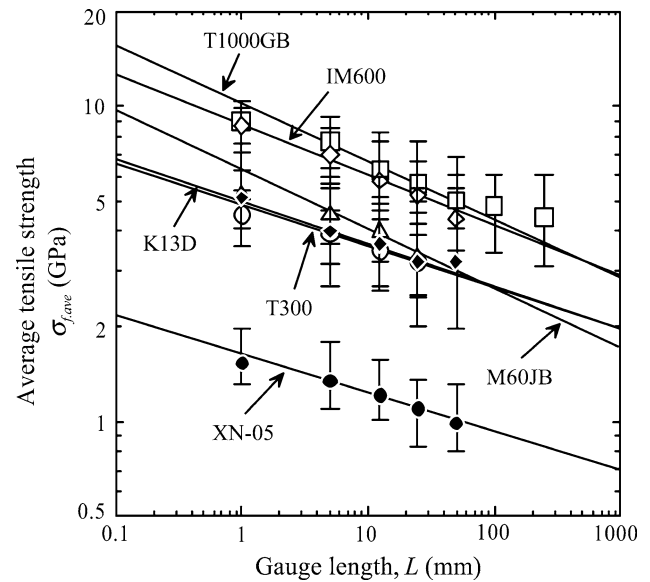

Fig. 5 Relation between the average tensile strength and the gauge length of PAN- and pitch-based carbon fibers. *Open circle* T300, *open square* T1000GB, *open diamond* IM600, *open triangle* M60JB PAN-based and *filled circle* XN-05, *filled diamond* K13D pitch-based carbon fibers. The m_f^* obtained from the Eq. 7. $m_f^* = 7.63$ (T300), 5.48 (T1000GB), 6.27 (IM600), 5.31 (M60JB), 8.23 (XN-05), and 7.36 (K13D)

From Eqs. 5 and 9, the Weibull modulus is modified

$$m_{\mathrm{f}} = \left(\frac{\sigma_{\mathrm{f.ave}}}{\sigma_0}\right)^{-\alpha \cdot m_{\mathrm{f}}^*} \tag{10}$$

Rearrangement of the Eq. 10 gives the following:

$$\ln(m_{\mathrm{f}}) = -\alpha \cdot m_{\mathrm{f}}^* \ln(\sigma_{\mathrm{f.ave}}) + \alpha \cdot m_{\mathrm{f}}^* \ln(\sigma_0) \tag{11}$$

Hence the linear relationship between the Weibull modulus, m_{f} and the average tensile strength, $\sigma_{\mathrm{f.ave}}$ can be obtained. Similar equations were referred as the "Power Law Accelerated Weibull" (PLAW) model [9, 28, 29]. The length scaling of the strength and the fixed length distribution are controlled by the different parameters.

Figure 6 shows the relation between the Weibull modulus, m_{f} and the average tensile strength, $\sigma_{\mathrm{f.ave}}$ of ultrahigh tensile strength PAN-based (T1000GB, IM600), ultrahigh tensile modulus pitch-based (K13D), high ductility pitch-based (XN-05), high strength PAN-based (T300), and high modulus PAN-based (M60JB) carbon fibers. For each type of carbon fiber, the Weibull modulus increased with increasing the average tensile strength. There is a linear relation between the Weibull modulus and the average tensile strength on log–log scale.

Obviously, the slop, $-\alpha \, m_{\mathrm{f}}^*$ depended on the strength, modulus, and structure of the carbon fibers. The highest

Fig. 6 Relation between the Weibull modulus and the average tensile strength of PAN- and pitch-based carbon fibers. *Open circle* T300, *open square* T1000GB, *open diamond* IM600, *open triangle* M60JB PAN-based and *filled circle* XN-05, *filled diamond* K13D pitch-based carbon fibers. $-\alpha \, m_{\mathrm{f}}^* = 0.89$ (T300), 1.23 (T1000GB), 1.20 (IM600), 0.87 (M60JB), 0.30 (XN-05), and 0.94 (K13D)

$|-\alpha \, m_{\mathrm{f}}^*|$ was observed for the ultrahigh strength T1000GB PAN-based fiber and the lowest $|-\alpha \, m_{\mathrm{f}}^*|$ was observed for the high ductility XN-05 pitch-based fiber. The $|-\alpha \, m_{\mathrm{f}}^*|$ of ultrahigh strength T1000GB PAN-based fiber was higher than that of high strength T300 PAN-based fiber and it was clear observed the strength dependence of the slop. The $|-\alpha \, m_{\mathrm{f}}^*|$ of the high modulus M60JB PAN-based fiber was almost similar to that of the high strength T300 PAN-based fiber (modulus dependence). The $|-\alpha \, m_{\mathrm{f}}^*|$ of the ultrahigh modulus K13D pitch-based fiber was higher than that of the high modulus M60JB PAN-based fiber (structure dependence).

In addition, for ultrahigh tensile strength T1000GB PAN-based, high ductility XN-05 pitch-based and high strength T300 PAN-based carbon fibers, the Weibull modulus of flexural strength versus average flexural strength was almost on the line obtained from the Eq. 11. However, for ultrahigh tensile modulus K13D pitch-based and high modulus M60JB PAN-based carbon fibers, the Weibull modulus of flexural strength versus average flexural strength was not on the line and the flexural strength of K13D and M60JB fibers was much lower than their tensile strength.

Afferrante et al. [30] discussed the implications of interactions between the cracks on variations in the Weibull modulus analytically using an efficient dual boundary element method (DBEM) and the Weibull modulus could vary because of interaction between the cracks (defects) or between the cracks and the stress field. This effect is one of the main reasons for the differences in the Weibull modulus of each fibers, the Weibull modulus at various gauge lengths and the Weibull modulus under tensile and flexural strength in this study.

Concluding remarks

The tensile properties of PAN-based (T1000GB, IM600, T300, and M60JB) and pitch-based (K13D and XN-05) single carbon fibers were performed at various gauge lengths ranging from 1 to 250 mm. The results are briefly summarized.

(1) The ultrahigh modulus pitch-based (K13D) carbon fiber has the lowest Weibull modulus at various gauge lengths ranging from 1 to 50 mm.

(2) The Weibull modulus and the average tensile strength increased with decreasing the gauge length and there is a linear relation between the Weibull modulus, the average tensile strength and the gauge length on log–log scale.

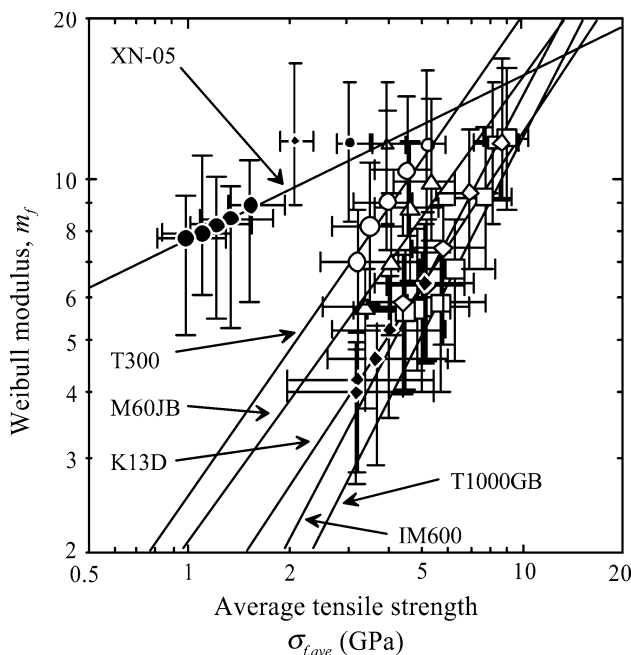(3) The Weibull modulus increased with increasing the average tensile strength and there is a linear relation

between the Weibull modulus and the average tensile strength on log–log scale.

References

1. Fitzer E (1989) Carbon 27(5):621. doi:10.1016/0008-6223(89)90197-8
2. Chand S (2000) J Mater Sci 35(6):1303. doi:10.1023/A:1004780301489
3. Rosa LG, Colella A, Anjinho CA (2006) Mater Sci Forum 514–516:672. doi:10.4028/www.scientific.net/MSF.514-516.672
4. Naito K, Tanaka Y, Yang JM, Kagawa Y (2008) Carbon 46(2):189. doi:10.1016/j.carbon.2007.11.001
5. Naito K, Tanaka Y, Yang JM, Kagawa Y (2009) J Am Ceram Soc 92(1):186. doi:10.1111/j.1551-2916.2008.02868.x
6. Johnson W (1985) In: Watt W, Perov BV (eds) Strong fibers, vol 1. Elsevier, Amsterdam, p 389
7. Thorne DJ (1974) Nature 248(5451):754. doi:10.1038/248754a0
8. Stoner EG, Edie DD, Durham SD (1994) J Mater Sci 29(24):6561. doi:10.1007/BF00354022
9. Padgett WJ, Durham SD, Mason AM (1995) J Compos Mater 29(14):1873. doi:10.1177/002199839502901405
10. Tagawa T, Miyata T (1997) Mat Sci Eng A Struct 238(2):336. doi:10.1016/S0921-5093(97)00454-1
11. Pickering KL, Murray TL (1999) Compos Part A Appl S 30(8):1017. doi:10.1016/S1359-835X(99)00003-2
12. Paiva MC, Bernardo CA, Nardin M (2000) Carbon 38(9):1323. doi:10.1016/S0008-6223(99)00266-3
13. Jones JB, Barr JB, Smith RE (1980) J Mater Sci 15(10):2455. doi:10.1007/BF00550747
14. Asloun EM, Donnet JB, Guilpain G, Nardin M, Schultz J (1989) J Mater Sci 24(10):3504. doi:10.1007/BF02385732
15. ASTM C1557-03 (2008) In: ASTM Annual Book of Standards, vol 15.01. American Society for Testing and Materials, West Conshohocken. doi:10.1520/C1557-03R08
16. Sung MG, Sassa K, Tagawa T, Miyata T, Ogawa H, Doyama M, Yamada S, Asai S (2002) Carbon 40(11):2013. doi:10.1016/S0008-6223(02)00059-3
17. Morimoto T, Nakagawa S, Ogihara S (2005) JSME Int J Series A 48(4):194. doi:10.1299/jsmea.48.194
18. Weibull W (1951) J Appl Mech 18:293
19. Lu CS, Danzer R, Fischer FD (2002) J Am Ceram Soc 85(6):1640. doi:10.1111/j.1151-2916.2002.tb00330.x
20. Danzer R (2006) J Eur Ceram Soc 26(15):3043. doi:10.1016/j.jeurceramsoc.2005.08.021
21. ASTM C1239-07 (2009) ASTM Annual Book of Standards, vol 15.01. American Society for Testing and Materials, West Conshohocken. doi:10.1520/C1239-07
22. Rosa LG, Figueiredo I (2010) Mater Sci Forum 636–637:1443. doi:10.4028/www.scientific.net/MSF.636-637.1443
23. Davies IJ (2004) J Mater Sci 39(4):1441. doi:10.1023/B:JMSC.0000013913.84004.cd
24. Absi J, Fournier P, Glandus JC (1999) J Mater Sci 34(6):1219. doi:10.1023/A:1004561023528
25. Trustrum K, Jayatilaka ADK (1979) J Mater Sci 14(5):1080. doi:10.1007/BF00561290
26. Pan N, Chen HC, Thompson J, Inglesby MK, Khatua S, Zhang XS, Zeronian SH (1997) J Mater Sci 32(10):2677. doi:10.1023/A:1018679207303
27. Wilson DM (1997) J Mater Sci 32(10):2535. doi:10.1023/A:1018538030985
28. Curtin WA (2000) J Compos Mater 34(15):1301. doi:10.1177/002199830003401503
29. Watson AS, Smith RL (1985) J Mater Sci 20(9):3260. doi:10.1007/BF00545193
30. Afferrante L, Ciavarella M, Valenza E (2006) Int J Solids Struct 43(17):5147. doi:10.1016/j.ijsolstr.2005.08.002